Potential of asymmetrical Si/Ge and Ge/Si based hetero-junction transit time devices over homo-junction counterparts for generation of high power

Moumita Mukherjee[1, †], Pravash R. Tripathy[2], and S. P. Pati[3, †]

[1]Centre of Millimeter-Wave Semiconductor Devices and Systems, Institute of Radio Physics and Electronics, University of Calcutta, 1, Girish Vidyaratna Lane, Kolkata 700009, West Bengal, India
[2]Puroshottam Institute of Engineering & Technology, Rourkela, Odisha, India, Sambalpur University, India
[3]AICTE Emeritus Professor, NIST, Pelur Hills, Berhampur, Odisha, India

Abstract: Static and dynamic properties of both complementary n-Ge/p-Si and p-Ge/n-Si hetero-junction Double-Drift IMPATT diodes have been investigated by an advanced and realistic computer simulation technique, developed by the authors, for operation in the Ka-, V- and W-band frequencies. The results are further compared with corresponding Si and Ge homo-junction devices. The study shows high values of device efficiency, such as 23%, 22% and 21.5%, for n-Ge/p-Si IMPATTs at the Ka, V and W bands, respectively. The peak device negative conductances for n-Si/p-Ge and n-Ge/p-Si hetero-junction devices found to be 50.7×10^6 S/m^2 and 71.3×10^6 S/m^2, which are $\sim$3–4 times better than their Si and Ge counterparts at the V-band. The computed values of RF power-density for n-Ge/p-Si hetero-junction IMPATTs are 1.0×10^9, 1.1×10^9 and 1.4×10^9 W/m^2, respectively, for Ka-, V- and W-band operation, which can be observed to be the highest when compared with Si, Ge and n-Si/p-Ge devices. Both of the hetero-junctions, especially the n-Ge/p-Si hetero-junction diode, can thus become a superior RF-power generator over a wide range of frequencies. The present study will help the device engineers to choose a suitable material pair for the development of high-power MM-wave IMPATT for applications in the civil and defense-related arena.

Key words: admittance characteristics; double drift diode; high-power IMPATT; high-efficiency; MM-wave device; Si/Ge and Ge/Si material systems

DOI: 10.1088/1674-4926/32/11/113001 **EEACC:** 2520

1. Introduction

Present-day communication systems demand the use of RF signals in the microwave and MM-wave frequency band owing to their higher resolution and broader bandwidth. The advance in solid-state devices has contributed significantly to the feasibility of high-power MM-wave sources. Among all the semiconductor devices, IMPATT diodes are considered as the most promising high-power devices. Increased demand for high-power and high-frequency applications in defense and the commercial arena have geared up research activities on IMPATT diodes. In recent years, several semiconductor materials, such as InP, SiC, ZnS and GaN, have been proposed for the fabrication of high-power MM-wave IMPATT diodes[1−4]. Even though this new class of semiconductor based IMPATTs has certain advantages, experimental success is limited due to difficulties of pure crystalline material growth techniques for p and n type layers and a lack of established fabrication and ohmic contact technologies. On the other hand, Si technology has already reached a fair level of maturity. Moreover, compared with SiC, InP and GaN wafers, Si wafers are easily available and cost effective. This is why semiconductor devices fabricated on Si have dominated the solid-state electronics industry for the last three decades. The main drawbacks of conventional Si IMPATTs are their low power output and low efficiency in the higher MM-wave region. In this paper, we have proposed a way to solve this problem by using a material pair, which has distinctly different band gap energy and tolerable lattice mismatching, for developing DDR IMPATT diodes. In recent times, research and development of a Si/Ge hetero-junction based device has been reported[5]. The advance in semiconductor technology has made it possible to grow a thin multi layer device leading to the concept of hetero-junction devices.

The simulation of the dynamic properties of n-Si/p-Ge as well as p-Si/n-Ge asymmetrical hetero-junction IMPATTs along with Si and Ge homo-junction IMPATTs are studied and compared via a generalized simulation technique that we have developed. To the best of our knowledge, this is the first report of hetero-junction IMPATT diodes based on Si/Ge material systems.

2. Device modeling scheme

The IMPATT diode is basically a p–n junction diode that operates when it is reverse-biased to avalanche breakdown conditions. A schematic diagram of a hetero-junction IMPATT is shown in Fig. 1. A one-dimensional model of the p–n junction has been considered in the present analysis. The following assumptions have been made in the simulation of DC and small signal behavior of the double drift region (DDR) IMPATT diodes: (1) the electron and hole velocities have been taken to be saturated considering an appropriate punch through factor and thus independent of the electric field throughout the space-charge layer, (2) the effect of carrier space-charge has

† Corresponding author. Email: mou_mita_m@yahoo.com, mukherjee_mita@hotmail.com, prof_sppati@yahoo.co.in
Received 23 April 2011, revised manuscript received 15 June 2011 © 2011 Chinese Institute of Electronics

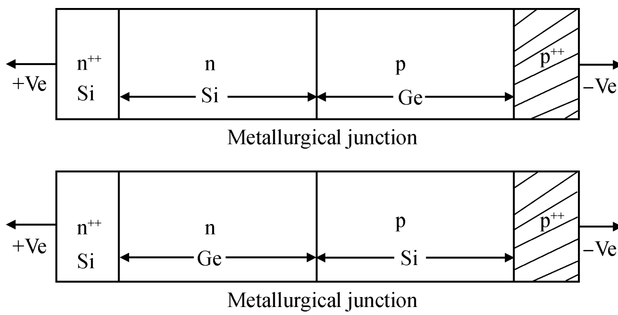

Fig. 1. Schematic diagram of heterojunction Si/Ge and Ge/Si IMPATTs at W-band.

been considered, (3) the effect of carrier diffusion has been considered, and (4) the effect of parasitic resistance is incorporated into the analysis.

2.1. DC analysis

The DC method, described in detail elsewhere[6], considers a generalized ($n^{++}npp^{++}$) structure. Here, n^{++} and p^{++} are highly doped substrates and n and p are epilayers. Summarily, in the DC method, the computation starts from the field maximum near the metallurgical junction. The distribution of dc electric field and carrier currents in the depletion layer are obtained by a double-iterative simulation method, which involves iteration over the magnitude of the field maximum (E_m), and its location near the junction within the depletion layer. The method is used for the simultaneous solution of Poisson and carrier continuity equations at each point in the depletion layer. The field boundary conditions are given by

$$E(-x_1) = 0, \quad E(+x_2) = 0. \tag{1}$$

Here, $-x_1$ and x_2 represent the edges of the depletion layer in the n and p regions, respectively.

The boundary conditions for normalized current density $P(x)$ are given by

$$P(-x_1) = (1/M_p - 1), \quad P(x_2) = (1 - 1/M_n). \tag{2}$$

$M_n = J/J_{ns}$, $M_p = J/J_{ps}$, where J_{ns} and J_{ps} are electron and hole leakage current densities, respectively. M_p and M_n are hole and electron current multiplication factors, respectively.

$P = (J_p - J_n)/J$, where J_p = hole current density, J_n = electron current density and J = total current density.

Thus the DC field and carrier current profiles are obtained by solving Poisson and carrier continuity equations, when boundary conditions (1) and (2) are satisfied. The realistic field dependence of electron and hole ionization rates, carrier mobility and the saturated drift velocities of electron ($v_{s,n}$) and hole ($v_{s,p}$) in Si and Ge[7, 8] are used in the computation of the profiles of electric field and carrier currents.

The RF conversion efficiency (η)[9] is calculated from the semi-quantitative formula,

$$\eta\,(\%) = 100V_D/\pi V_B, \tag{3}$$

where V_D = voltage drop across the drift region. Also, $V_D = V_B - V_A$, where V_A = voltage drop across the avalanche region and V_B = breakdown voltage.

The results of the DC analysis are then used in the small signal analysis, described briefly in the next sub-section.

2.2. Small signal RF-analysis

The small signal analysis of the IMPATT diode provides insight into the high frequency performance of the diode. The range of frequencies exhibiting negative conductance of the diode can easily be computed by the Gummel-Blue method[10]. From the dc field and current profiles, the spatially dependent ionization rates that appear in the Gummel-Blue equations are evaluated, and fed as input data into the small signal analysis. The edges of the depletion layer of the diode, which are fixed by the dc analysis, are taken as the starting and end points for the small signal analysis. On splitting the diode impedance $Z(x,\omega)$ obtained from the Gummel–Blue method, into its real part $R(x,\omega)$ and imaginary part $X(x,\omega)$, two differential equations are framed[11, 12]. A double-iterative simulation scheme incorporating a modified Runge-Kutta method is used to solve these two equations simultaneously. The small signal integrated parameter, like negative conductance ($-G$), susceptance (B), impedance (Z), frequency band width, and the quality factor (Q) of the diode, are obtained, satisfying the boundary conditions derived elsewhere[11].

The simulation method provides the high-frequency negative resistance and negative reactance profiles in the space-charge layer of the device. The diode negative resistance ($-Z_R$) and reactance ($-Z_X$) are computed through numerical integration of the $-R(x)$ and $-X(x)$ profiles over the active space-charge layer.

Thus

$$Z_R = -\int_{-x_2}^{x_2} R\mathrm{d}x, \tag{4}$$

and

$$Z_X = -\int_{-x_2}^{x_2} X\mathrm{d}x. \tag{5}$$

The diode impedance Z is given by

$$Z(\omega) = -\int_{-x_2}^{x_2} Z(x,\omega) = -Z_R + \mathrm{j}Z_X. \tag{6}$$

The diode admittance is expressed as

$$Y = 1/Z = -G + \mathrm{j}B = 1/(-Z_R + \mathrm{j}Z_X), \tag{7}$$

where $-G = -Z_R/(Z_R^2 + Z_X^2)$ and $B = Z_X/(Z_R^2 + Z_X^2)$.

It may be noted that both $-G$ and B are normalized to the area of the diode.

The avalanche frequency (f_a) is the frequency at which the imaginary part, susceptance (B) of the admittance changes its nature from inductive to capacitive. Again, it is the minimum frequency at which the real part, conductance (G) of the admittance becomes negative. At the avalanche frequency, oscillation starts to build up in the circuit.

The small signal quality factor (Q) is defined as the ratio of the imaginary part of the admittance to the real part of the admittance (at the peak frequency), i.e., $-Q_p = (B_p/-G_p)$.

Table 1. Design parameters of Si, Ge, Si/Ge and Ge/Si based MM-wave IMPATTs.

Design frequency band	Structural parameters	Si (Homo-junction)	Ge (Homo-junction)	(n-)Si/(p-)Ge (Hetero-junction)	(n-)Ge/(p-)Si (Hetero-junction)
Ka band	Background doping concentration (n-side) (10^{22} m^{-3})	2.7	2.0	3.0	5.0
	Background doping concentration (p-side)(10^{22} m^{-3})	3.3	2.0	4.5	3.0
	Depletion region width (n-side) (μm)	1.5	1.0	0.50	0.48
	Depletion region width (p-side) (μm)	1.5	1.0	0.48	0.50
	Bias current density (10^7 A/m^2)	3.5	4.0	1.0	1.0
	Substrate doping concentration (10^{26} m^{-3})	1.0	1.0	1.0	1.0
V band	Background doping concentration (n-side) (10^{22} m^{-3})	7.0	3.8	7.5	9.0
	Background doping concentration (p-side) (10^{22} m^{-3})	7.8	3.8	9.0	8.0
	Depletion region width (n-side) (μm)	0.5	0.6	0.25	0.25
	Depletion region width (p-side) (μm)	0.5	0.6	0.25	0.25
	Bias current density (10^7 A/m^2)	7.0	7.0	5.0	5.0
	Substrate doping concentration (10^{26} m^{-3})	1.0	1.0	1.0	1.0
W band	Background doping concentration (n-side) (10^{22} m^{-3})	13.0	8.0	18.0	16.0
	Background doping concentration (p-side) (10^{22} m^{-3})	16.0	8.5	23.0	12.0
	Depletion region width (n-side) (μm)	0.3	0.26	0.13	0.15
	Depletion region width (p-side) (μm)	0.25	0.25	0.13	0.18
	Bias current density (10^7 A/m^2)	8.0	8.0	10.0	10.0
	Substrate doping concentration (10^{26} m^{-3})	1.0	1.0	1.0	1.0

At a given bias current density, the peak frequency (f_p) is the frequency at which the negative conductance of the diode is at a maximum, and the quality factor is at a minimum.

At resonance, the maximum RF power output (P_{RF}) from the device is obtained from the expression[13] $P_{RF} = (V_{RF}{}^2 G_P)/2$, where V_{RF} (amplitude of the RF swing) is taken as $V_B/2$, assuming a 50% modulation of the breakdown voltage V_B. The diode negative conductance at the optimum frequency ($-G_p$) is normalized to the area of the diode. The role of parasitic positive series resistance is also considered for calculating realistic values of P_{RF}.

3. Results and discussions

The structural parameters of MM-wave optimized diodes are shown in Table 1. Background doping concentrations and current densities are optimized for an appropriate punch-through factor[12]. The electric field profiles of the diodes at Ka band, V band and W band are shown in Figs. 2(a)–2(c). It is observed from the figures that in each case, the electric field maximum in homo-junction Si IMPATTs is higher than in other diodes. The same observation is reflected in Table 2, where the DC and high-frequency properties of the different IMPATT diodes at the Ka band, V band and W band are depicted. It is also observed that the breakdown voltages in Si homo-junction devices are 35 V, 19 V and 17 V, respectively at the Ka band, V band and W band. These values are higher than its Ge, n-Si/p-Ge and n-Ge/p-Si counterparts. However, it is very interesting to note that in the case of n-Si/p-Ge and n-Ge/p-Si hetero-junction diodes, the voltage across the avalanche region (V_a) has been decreased significantly. It is found that in Si and Ge homo-junction diodes, V_a are 24 V and 15.6 V at the Ka band, 13.5 V and 10.1 V at the V band and 8.5 V and 6.1 V at the W band. Whereas in the case of n-Si/p-Ge and n-Ge/p-Si diodes, it decreases to 9.1 V, 5.35 V at the Ka band, 5.45 V, 3.93 V at the V band and 3.3 V and 2.8 V at the W band. If one observes the electron and hole ionization rate in silicon and germanium, the hole ionization rate in Ge is observed to be considerably higher compared with the other three corresponding values. The x_a/W and V_a in the case of a n-Ge/p-Si hetero junction becomes the minimum as a high value of hole ionization rate in Ge augments the charge multiplication process and therefore localizes the avalanche zone in the hole initiated n-Ge layer of this hetero junction. This reduction of V_a increases the drift voltage drop in the case of hetero-junction IMPATTs, which in turn increases the efficiency. From the simulation studies, it is clear that in the case of hetero-junction diodes, the normalized drift voltage drop is quite a lot higher than its homo-junction coun-

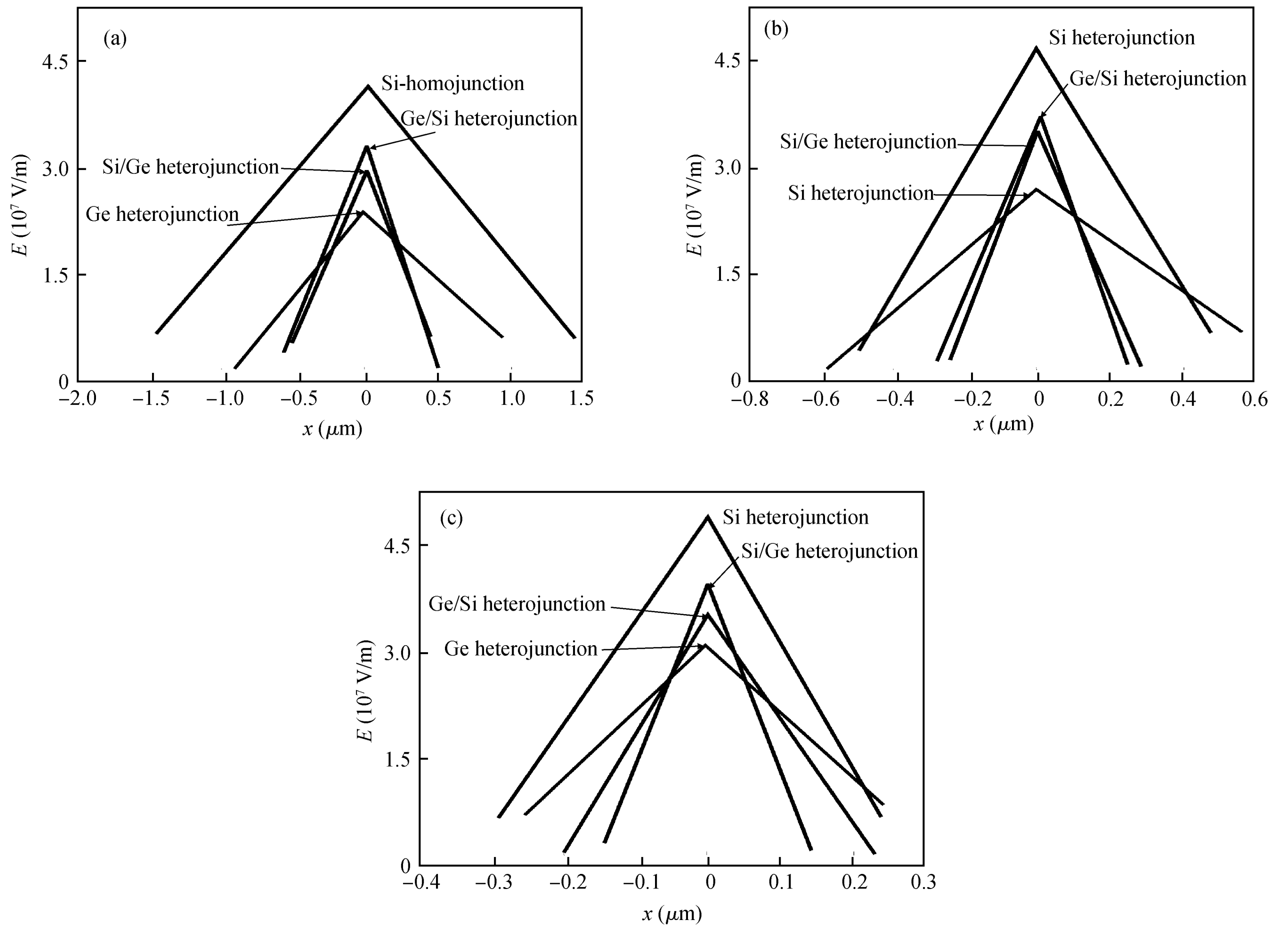

Fig. 2. Electric field profiles of heterojunction and homo-junction IMPATT diodes at (a) Ka band, (b) V band, and (c) W band.

Table 2. Simulation results of MM-wave homo-junction and hetero-junction IMPATT diodes

Design frequency band	DDR IMPATTs based on	DC results					High-frequency results					
		V_B (V)	V_a (V)	V_D/V_B (%)	E_{max} (10^7 V/m)	η (%)	f_P (GHz)	$-G_P$ (10^6 S/m^2)	$-Q_P$	P_{max} (10^9 W/m^2)	$-Z_{RP}$ (10^{-8} Ω·m^2)	$+R_S$ (10^{-8} Ω·m^2)
Ka-band	Si (Homo-junction)	35.0	24.0	31.4	4.10	10.0	36.5	6.5	1.2	1.0	5.1	0.55
	Ge (Homo-junction)	29.4	15.6	47.0	2.4	14.9	39.0	5.63	2.1	0.61	3.2	0.58
	(n-)Si/(p-)Ge (Hetero-junction)	18.0	9.1	50.0	3.0	16.0	30.0	14.0	1.6	0.6	2.0	0.23
	(n-)Ge/(p-)Si (Hetero-junction)	18.7	5.35	71.3	3.14	23.0	28.0	23.0	0.3	1.05	4.1	0.75
V-band	Si (Homo-junction)	19.0	13.5	28.0	4.63	9.5	63.0	20.0	2.5	0.9	0.57	0.23
	Ge (Homo-junction)	18.7	10.1	46.0	2.7	14.6	62.0	14.2	2.3	0.6	1.14	0.204
	(n-)Si/(p-)Ge (Hetero-junction)	10.4	5.45	47.0	3.4	15.2	66.0	50.7	1.4	0.7	0.65	0.145
	(n-)Ge/(p-)Si (Hetero-junction)	10.6	3.93	63.0	3.47	22.0	68.0	71.3	1.1	1.1	0.66	0.188
W-band	Si (Homo-junction)	17.0	8.5	29.23	4.85	9.3	94.5	27.0	4.1	0.9	2.1	0.70
	Ge (Homo-junction)	9.88	6.07	38.56	3.07	12.3	94.0	19.5	6.5	0.24	1.0	0.16
	(n-)Si/(p-)Ge (Hetero-junction)	6.12	3.27	46.57	4.03	14.8	94.0	155.0	1.4	0.80	2.04	0.5
	(n-)Ge/(p-)Si (Hetero-junction)	8.62	2.80	67.52	3.86	21.5	94.0	164.0	0.7	1.4	4.86	2.41

terparts. It is found that in n-Si/p-Ge and n-Ge/p-Si IMPATTs, the normalized drift voltage drops are 50%, 71.3% at the Ka band, 47.0%, 63.0% at the D band and 46.57% and 67.52% at the W band, which are significantly higher than those in Si and Ge homo-junction diodes, as shown in Table 2. It is observed from the comparative analysis that the RF conversion efficiency in Si IMPATTs is 10%, 9.5% and 9.3%, respectively for Ka-band, V-band and W-band operation, whereas the same

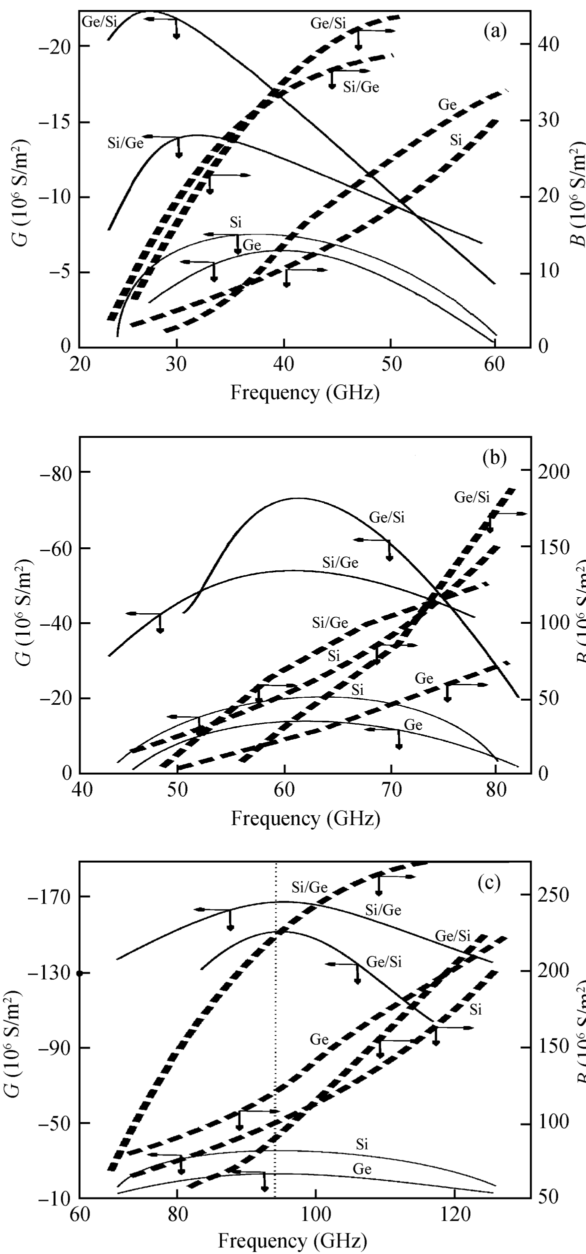

Fig. 3. Admittance plots of (a) Ka band, (b) V band and (c) W band hetero-junction and homo-junction IMPATTs. Junction temperature is 500 K.

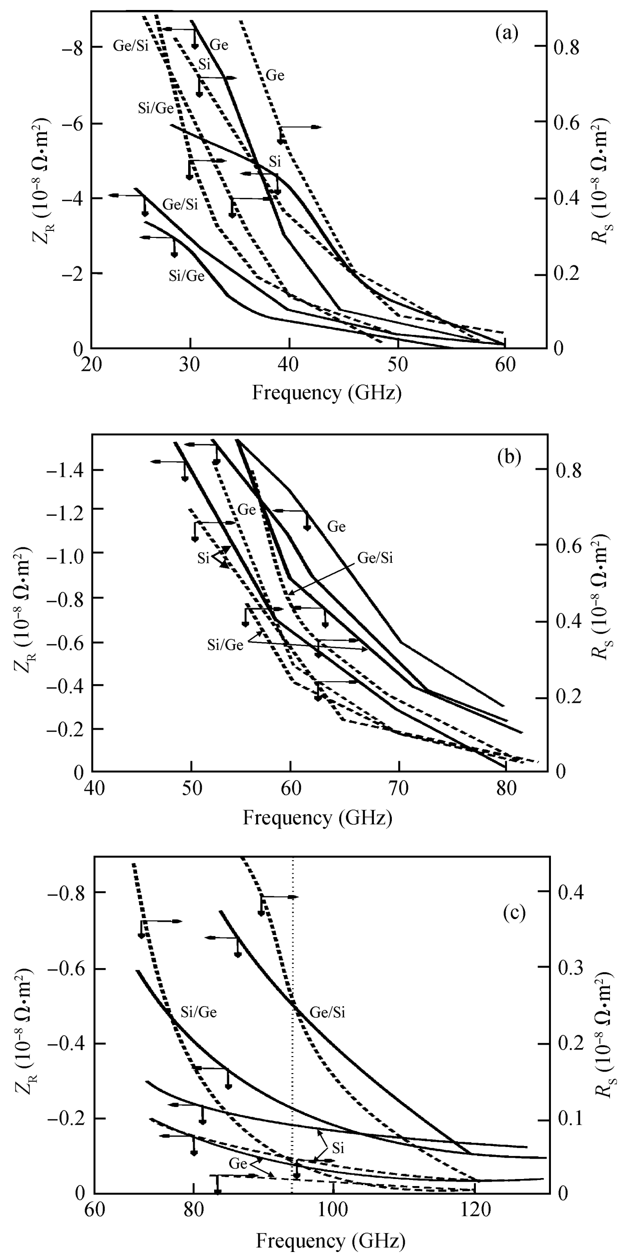

Fig. 4. Variation of negative resistance and parasitic resistance with frequency in (a) Ka band, (b) V band, and (c) W band homo-junction and hetero-junction IMPATTs. Junction temperature is 500 K.

in Ge IMPATTs are 14.9%, 14.6% and 12.3%, respectively for Ka-band, V-band and W-band operation. However, it increases to a much higher level in hetero-junction devices. The study depicts that for Ka-band operation, the device efficiencies are 16% and 23%, respectively, for n-Si/p-Ge and n-Ge/p-Si IMPATTs. For V-band operation, the same are 15.2% and 22%, and for W-band operation, they are 14.8% and $\sim$22%, in case of n-Si/p-Ge and n-Ge/p-Si IMPATTs. So, in terms of RF conversion efficiency, hetero-junction IMPATTs are performing much better than their homo-junction counterparts at all three important MM-wave frequency bands. Among the two complementary hetero junction DDs, the n-Ge/p-Si is expected to perform better than its counterpart.

Figures 3(a)–3(c) compare the admittance characteristics of all designed diodes at the Ka band, V band and W band. It is observed at all three frequency bands that negative conductance is much higher in hetero-junction diodes than in homo-junction diodes. Negative conductance of all the diodes increases initially up to the peak operating frequency, then it decreases as expected. Diode susceptance increases continuously with frequency. It is interesting to see from Table 2 that the quality factor of the diodes improves (decreases) significantly when we are using hetero-junction diodes. This indicates that in the MM-wave region, signal generation stability from hetero junction IMPATTs will be far better than their homo-junction counterparts. Negative resistances (Z_R) and parasitic positive resistances (R_S) of the devices are shown in Figs. 4(a)–4(c) for Ka-band, V-band and W-band devices. It is found that in the case of n-Ge/p-Si hetero-junction IMPATTs, device negative resistances are 4.10×10^{-8} Ω·m^2, 0.66×10^{-8} Ω·m^2 and

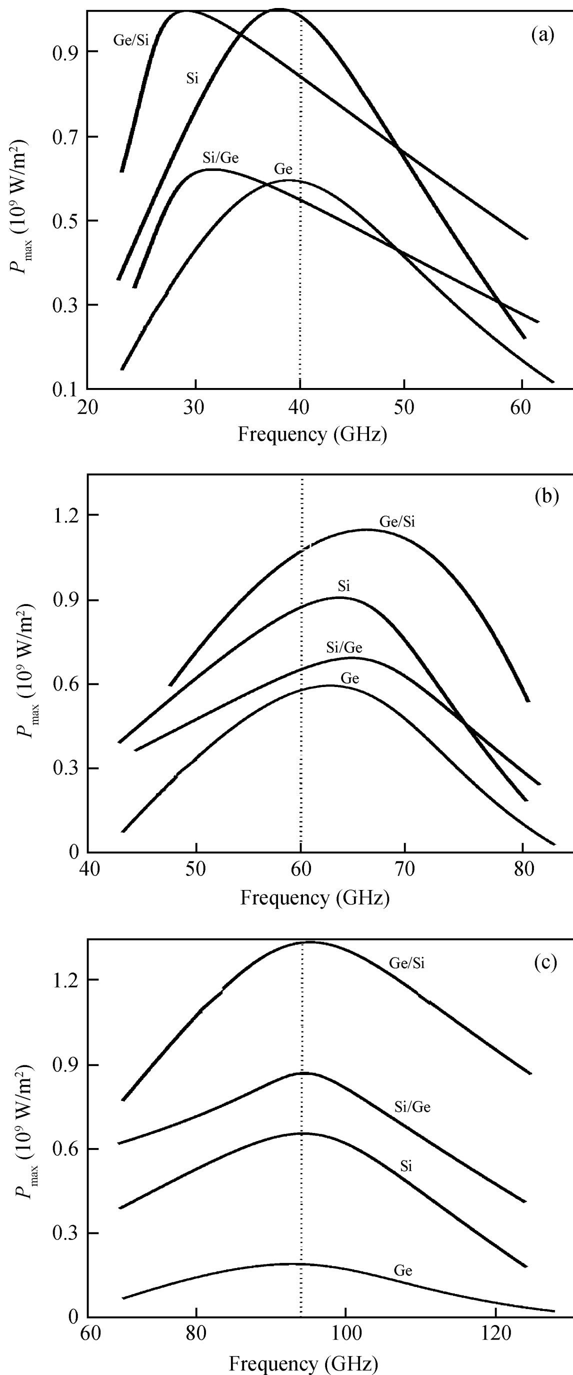

Fig. 5. Variation of RF power and frequency in hetero-junction and homo-junction DDR IMPATTs at (a) Ka band, (b) V band and (c) W band. Junction temperature is 500 K.

4.86×10^{-8} Ω·m^2, respectively for Ka-band, V-band and W-band devices—far better compared with their homo-junctions and other hetero-junction counterparts. It is interesting to observe that for high-frequency operation (W band), the negative resistance of the devices decreases significantly but n-Ge/p-Si hetero-junction IMPATTs still show a high value of negative resistance $\sim 4.86 \times 10^{-8}$ Ω·m^2. In the case of all the diodes, positive series resistance is found to be smaller compared with their negative resistances. This is an essential condition for oscillation to take place.

The variation in RF power with frequency for all the MM-wave diodes is shown in Figs. 5(a)–5(c). It is interesting to observe that n-Ge/p-Si hetero-junction IMPATTs may produce 1.0×10^9 W/m^2, 1.1×10^9 W/m^2 and 1.4×10^9 W/m^2 of RF power densities at the Ka band, V band and W band, which are much higher than Si, Ge and n-Si/p-Ge devices at the corresponding frequencies. Thus in terms of power output and efficiency, hetero-junction IMPATTs, particularly n-Ge/p-Si hetero-junction diodes are performing much better than others. The results mentioned here may provide due impetus for the fabrication of hetero junction IMPATTs for operation in the MM-wave range. Already some results have appeared in the literature that indicate this trend. The following section gives a proposed fabrication methodology.

4. Proposed fabrication techniques

A Si/Ge hetero-junction diode may be fabricated by depositing p-Ge thin films on n-Si substrates using molecular beam epitaxy and electron beam evaporation techniques[14]. The fabrication simplicity and absence of high-temperature diffusion processes may be taken as favorable parameters for n-Ge/p-Si hetero-junction devices for use as detectors in the visible and IR ranges: 500 to 1800 nm. Reports indicate that the crystal mismatch (about 4.2%) between Ge and Si can be reduced by varying the Ge proportion layer width in Ge_xSi_{1-x} and $Ge_{1-x}C_x$ combinations as well as by post-deposition thermal annealing[15]. Ge films (100–200 nm thick) can be deposited on n-type silicon substrates (ρ: 1.5–20 Ω·cm) by both E-beam evaporation (CHA: base pressure of 3×10^{-6} Torr), and molecular beam epitaxy (MBE: base pressure 8×10^{-6} Torr). The films were found to be p-doped (ρ: 0.06–1 Ω·cm), as grown. The growth temperature for MBE and E-beam evaporation is 375 ± 25 ℃ and 300 ± 10 ℃, respectively. The growth of Ge on Si, using MBE, can be monitored by reflection high energy electron diffraction (RHEED). The crystal quality and strain of grown Ge/Si structures is probed by *ex situ* X-ray diffraction (both θ–2θ and rocking curves) using CuKα_1 (1.5406 Å) radiation in a double-axis Bede3 diffractometer. The electrical and optical properties of both large (5×5 mm^2) and 200×200 μm^2 mesa p–n junctions have also been studied. Ohmic contacts are made on Si through Ti/Al and on Ge using silver and Au/Pd[16]. The etch pit density is significantly lower in the MBE samples (5×10^8 cm^{-2}) compared with E-beam samples (2×10^{10} cm^{-2}). The appreciable performance of the p–n junction diode is expected to provide a drive for fabrication of hetero-junction based IMPATT diodes.

5. Conclusion

This study throws light on the static and dynamic characteristics of Si, Ge, Si/Ge and Ge/Si IMPATT diodes. Both of the complementary hetero-junction diode structures may be taken as better RF generators compared to homo junction Si and Ge IMPATTs. It is observed that the MM-wave performance of n-Ge/p-Si hetero-junction IMPATTs may become the best and thus would be extremely useful for MM-wave power generation at Ka-band, V-band and W-band frequencies.

Acknowledgment

Moumita Mukherjee wishes to acknowledge DRDO, Ministry of Defense, Government of India for her "Research Associateship" to carry out this work. Prof. S. P. Pati wishes to express his sincere thanks to AICTE, New Delhi for the grant of Emeritus Fellowship in his favor. Preliminary results are presented and published in the Proceedings of the International IEEE Conference ICCCD-2010, at IIT-Kharagpur, India.

References

[1] Mukherjee M, Mazumder N, Dasgupta A. Simulation experiment on optical modulation of 4H-SiC millimeter-wave high power IMPATT oscillator. J European Microwave Association, 2008, 4: 276

[2] Mukherjee M, Mazumder N. Effect of charge-bump on high-frequency characteristics of α-SiC based double drift ATT diodes at MM-wave window frequencies. IETE Journal of Research, 2009, 55: 118

[3] Mukherjee M, Tripathy P, Pati S P. Effects of mobile space-charge on dynamic characteristics and parasitic resistance of InP terahertz IMPATT oscillator operating at elevated junction temperature. Archives of Applied Science Research, 2010, 2: 42

[4] Pati S P, Tripathy P R, Dash S K. Avalanche breakdown characteristics of wide band GaP vis-à-vis low band gap junctions and high RF power/low noise generation in ZnS DD IMPATTs. International Journal of Pure and Applied Physics, 2010, 6: 229

[5] Kanbe H, Miyaji M, Ito T. Ge/Si heterojunction photodiodes fabricated by low temperature wafer bonding. Appl Phys Express, 2008, 1: 072301

[6] Mukherjee M, Mazumder N, Roy S K, et al. GaN IMPATT diode: a photosensitive high power terahertz source. Semicond Sci Technol, 2007, 22: 1258

[7] Electronic archive: new semiconductor materials, characteristics and properties. [Online] http://www.ioffe.ru/SVA/NSM/Semicond/Si

[8] Mikawa T, Kagawa S, Kaneda T, et al. Fully ion-implanted p^{+}–n germanium avalanche photodiodes. Appl Phys Lett, 1981, 38: 429

[9] Scharfetter D L, Gummel H K. Large-signal analysis of a silicon Read diode oscillator. IEEE Trans Electron Devices, 1969, 16: 64

[10] Gummel H K, Blue J L. A small-signal theory of avalanche noise in IMPATT diodes. IEEE Trans Electron Devices, 1967, ED-14: 569

[11] Roy S K, Banerjee J P, Pati S P. A computer analysis of the distribution of high frequency negative resistance in the depletion layer of IMPATT diodes. Proc 4th Conf Num Anal Semiconductor Devices, Dublin, 1985: 494

[12] Pati S P, Tripathy P R, Dash S K, et al. Mathematical analysis and realistic simulation modeling for thin impact devices. Proc MATEIT, New Delhi, 2010

[13] Eisele H, Haddad G I. Microwave semiconductor device physics. Sze S M, ed. New York: Wiley, 1997: 343

[14] Bandaru P, Sahni S, Yablonovitch E, et al. The fabrication of p-Ge/n-Si photodetectors, compatible with back-end Si CMOS processing, by low temperature (< 400 ℃) molecular beam epitaxy and electron-beam evaporation. Mat Res Soc Symp Proc, 2004, 796: V2.8.1

[15] Bandaru P R, Sahni S, Yablonovitch E, et al. Fabrication and characterization of low temperature (< 450 ℃) grown p-Ge/n-Si photodetectors for silicon based photonics. Mater Sci Eng B, 2004, 113: 79

[16] Ismail R A, Koshapa J, Abdulrazaq O A. Ge/Si heterojunction photodetector for 1.064 mm laser pulses. International Journal of Semiconductor Physics, Quantum Electronics & Optoelectronics, 2006, 9: 49